Supplementary material

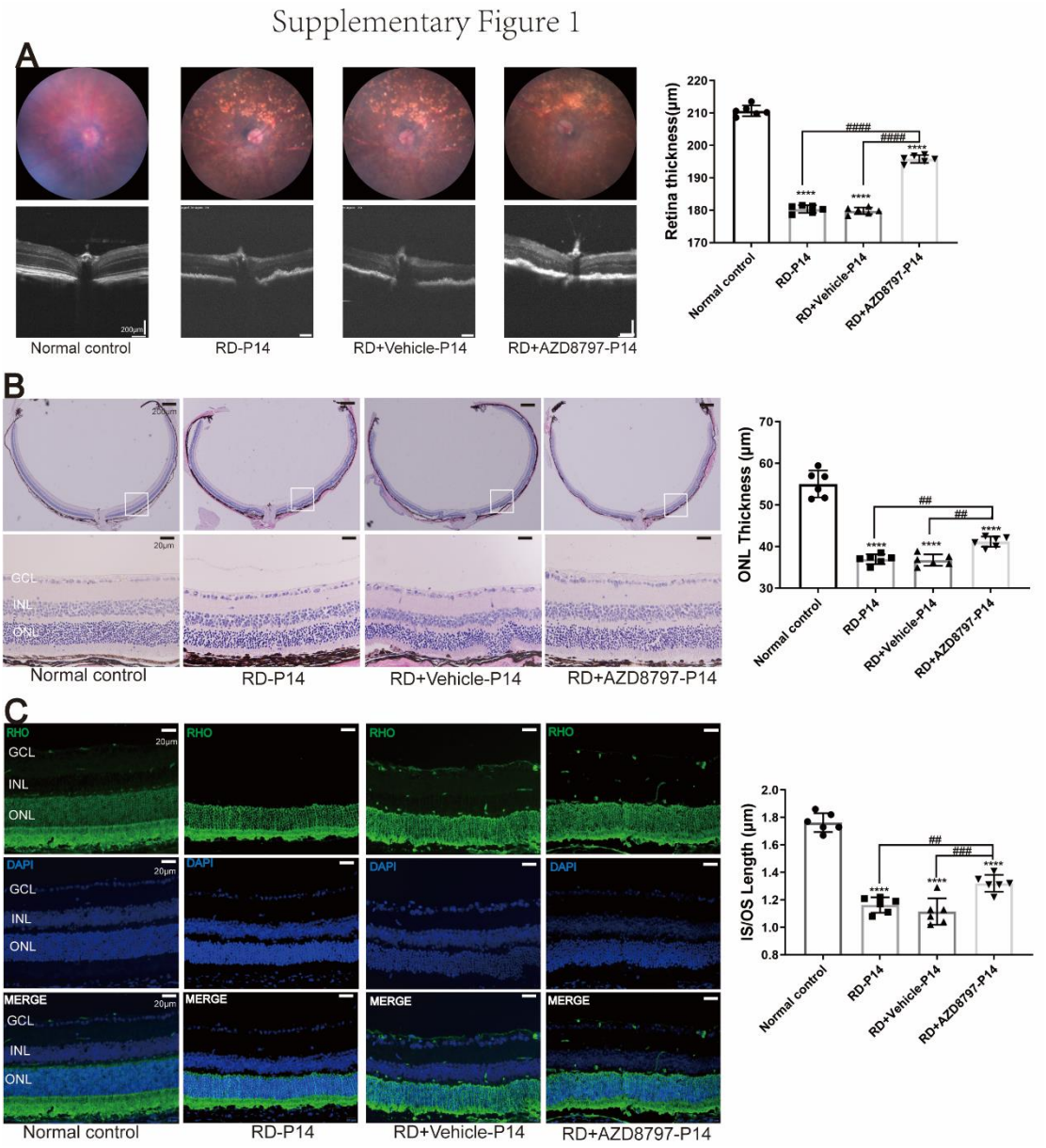

Supplementary FIGURE 1. AZD8797 alleviates the morphology damages in RD mice at P14

(A) Funds and OCT examination were performed at P14 to examine the AZD8797 mediated effects on retina morphology. **(B)**H&E staining was performed on the retinal sections at P14. Statistical results of ONL layer thickness after AZD8797 treatment. **(C)**Immunofluorescence staining of Rhodopsin in the retina of the AZD8797 treated mice; statistical analysis of the length of inner and outer segments. (*P < 0.05, **P < 0.01, ****P < 0.0001, for differences compared with the normal control, $^{\#}P$ < 0.05, $^{\#\#}P$ < 0.01, $^{\#\#\#}P$ < 0.001, $^{\#\#\#\#}P$ < 0.0001, for differences between animal groups, n = 6.)

Supplementary Figure 2

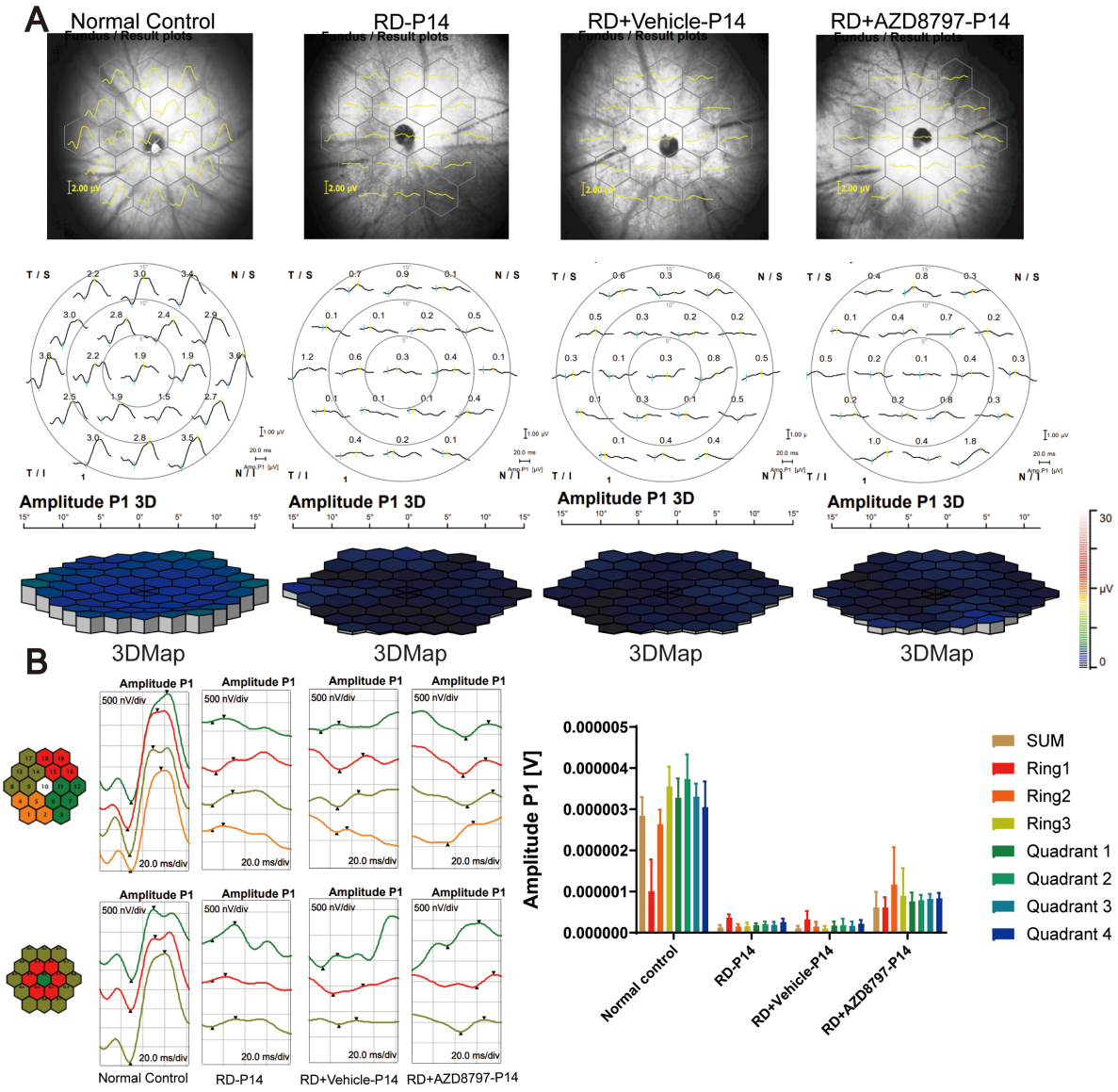

Supplementary FIGURE 2. AZD8797 preserved the retinal function in RD mice model at P14

(A) The typical ERG waveforms and 3D-ERG map animals after AZD8797 treatment at P14. **(B)**Representative images of amplitude changes in all the four quadrants: superior temporal, inferior and nasal quadrant, respectively, statistical analysis of the amplitudes in three recording rings: central, mid-pericentral, and peripheral ring, respectively.

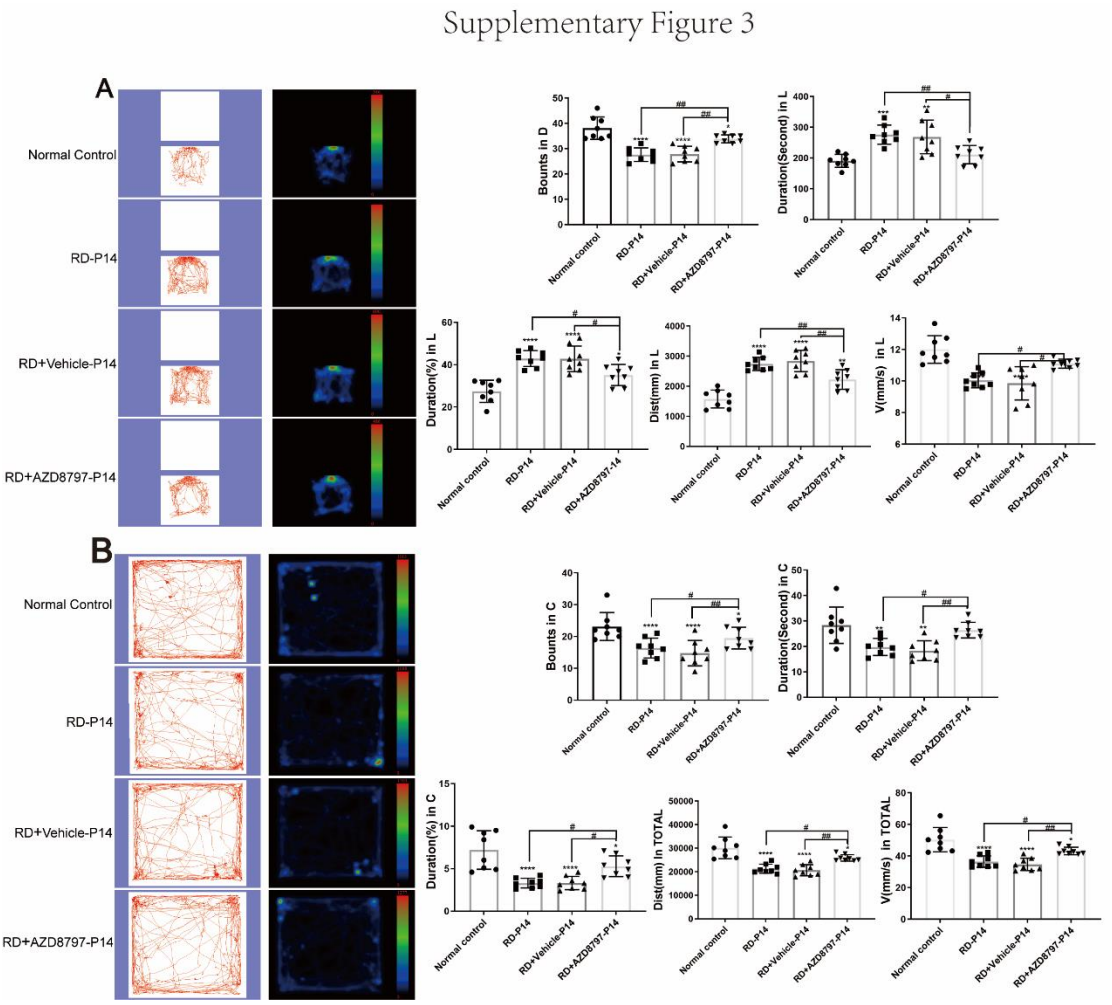

Supplementary FIGURE 3. AZD8797 mitigated the behavioral of RD model at P14.

(A) Light/dark box test (Trajectories and density maps) of the mice after AZD8797 treatment at P14; The statistical results of behavioral parameters including the shuttle through in dark box, durations in light box, the distance traveled in the light box, speed of movement of mice in light box; **(B)** Open filed test of (Trajectories and density maps) of the mice after AZD8797 treatment at P14. The statistical results of behavioral parameters including shuttle through in center area, durations(s) in center area, durations (%) in center area, the distance traveled in the center area, speed of movement of mice in center area. (*$P < 0.05$, **$P < 0.01$, ****$P < 0.0001$, for differences compared with the normal control, $^{\#}P < 0.05$, $^{\#\#}P < 0.01$, $^{\#\#\#\#}P < 0.0001$, for differences between animal groups, n = 8.)

Supplementary Figure 4

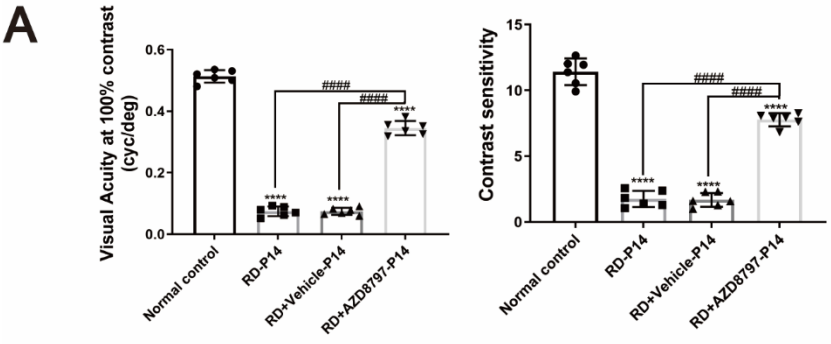

Supplementary FIGURE 4. AZD8797 improved visuospatial behavior in RD Model at P14

(A) Schematic diagram of visuospatial behavior test. **(B)**AZD8797 improved the spatial resolution and contrast sensitivity of RD model at P14. n = 6. (**P* < 0.05, ***P* < 0.01, *****P* < 0.0001, for differences compared with the normal control, $^{\#}P < 0.05$, $^{\#\#}P < 0.01$, $^{\#\#\#}P < 0.001$, $^{\#\#\#\#}P < 0.0001$ for differences between animal groups, n = 6.)

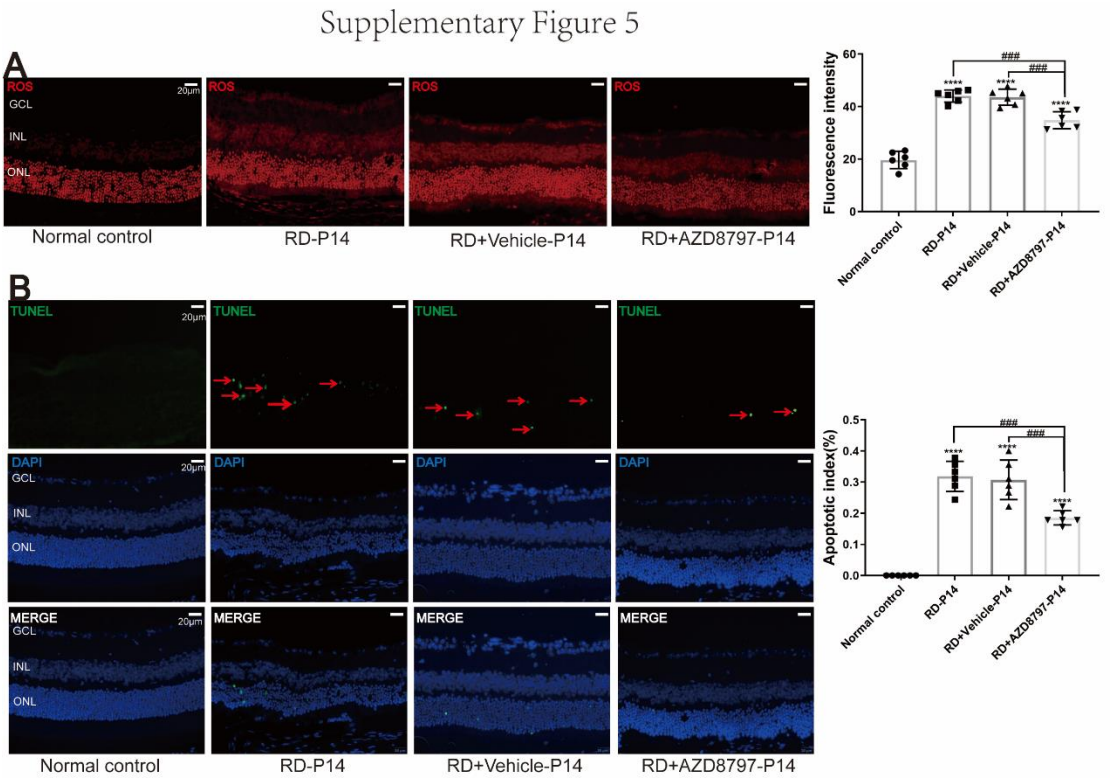

Supplementary FIGURE 5. AZD8797 ameliorate the oxidative stress and apoptosis in RD model at P14

(A)DHE fluorescence assay the ROS level after AZD8797 treatment at P14. **(B)**TUNEL staining to detect the number of apoptotic after AZD8797 treatment, the red arrows indicate TUNEL positive cells. (**P* < 0.05, ***P* < 0.01, *****P* < 0.0001, for differences compared with the normal control, $^{\#}P < 0.05$, $^{\#\#}P < 0.01$, $^{\#\#\#}P < 0.001$, $^{\#\#\#\#}P < 0.0001$, for differences between animal groups, n = 6.)

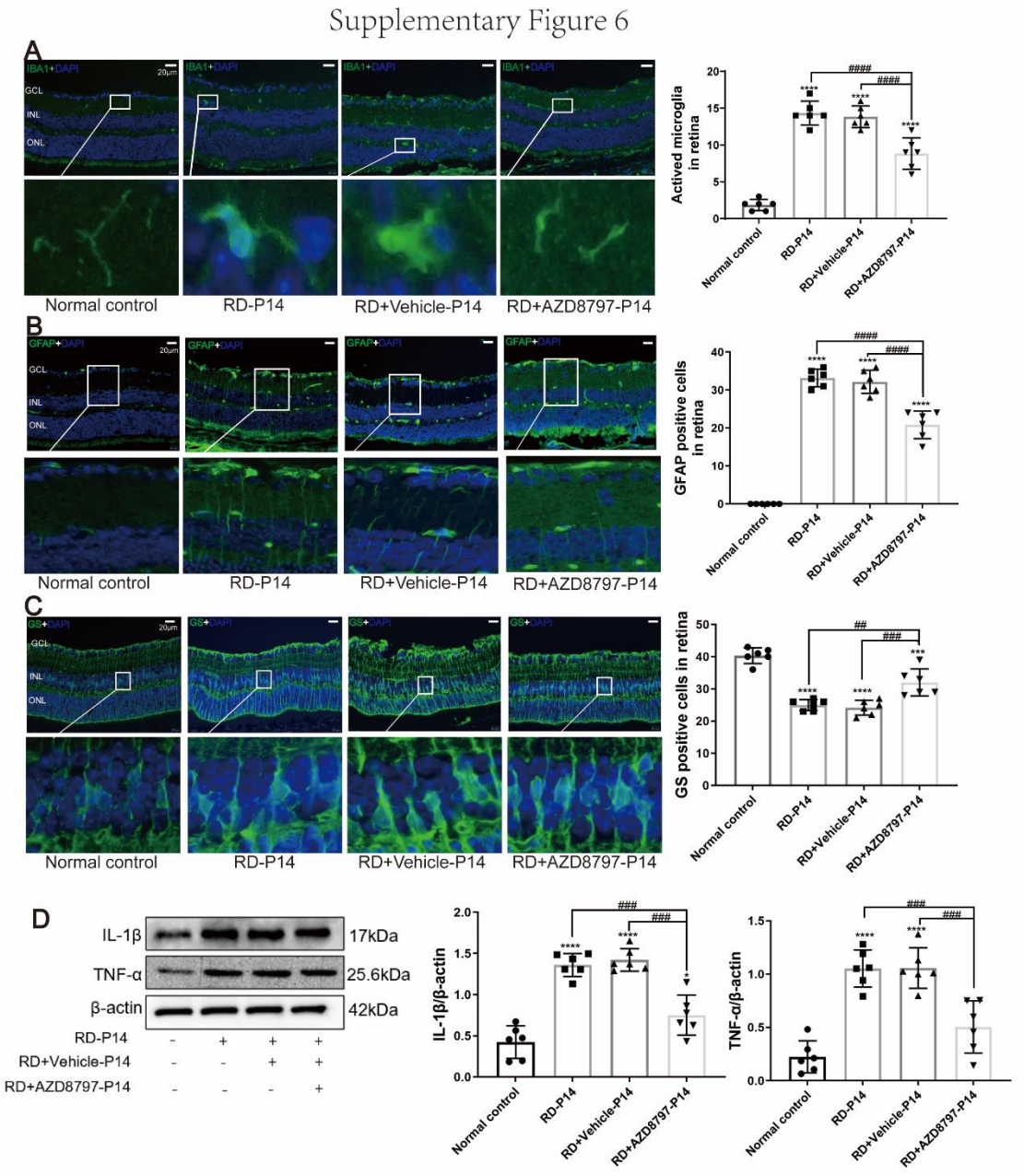

Supplementary FIGURE 6. AZD8797 inhibited the neuroglia activation and inflammatory response at P14

(A) Microglia labelled with IBA1 in the retinas after AZD8797 treatment at P14, as the white box marked. **(B)**Müller cell labelled with GFAP positive cells in the retinas after AZD8797 treatment as the white box indicated. **(C)** Müller cell labelled with GS in the retinas of the AZD8797 treated mice, as the white box marked. D. Western blot analysis of the IL-1β and TNF-α in the retinas of the AZD8797 treated mice. (Scale:20μm) (**P* < 0.05, ***P* < 0.01, *****P* < 0.0001, for differences compared with the normal control, $^{\#}P$ < 0.05, $^{\#\#}P$ < 0.01, $^{\#\#\#}P$ < 0.001, $^{\#\#\#\#}P$ < 0.0001, for differences between animal groups, n = 6.)

Supplementary Figure 7

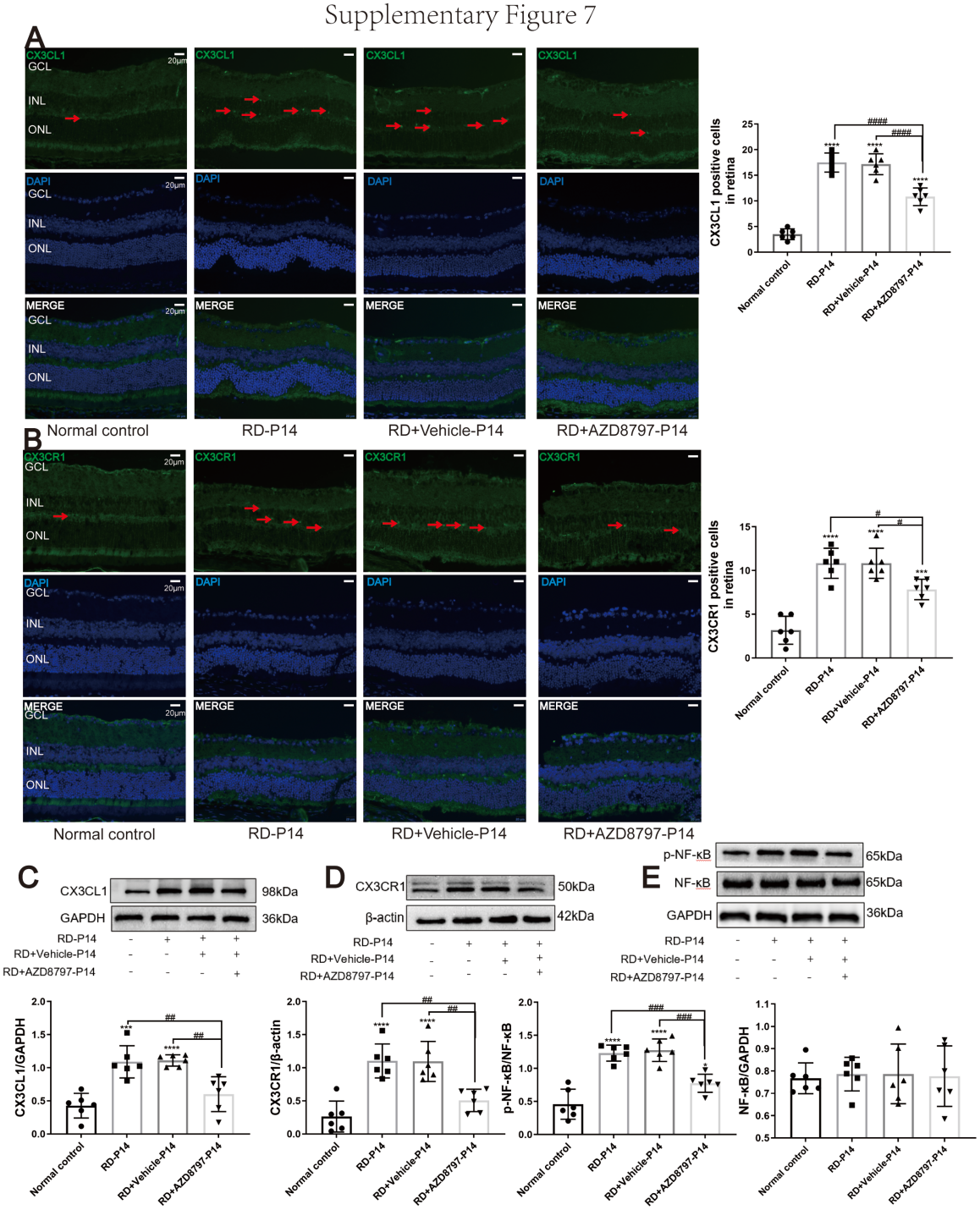

Supplementary FIGURE 7. AZD8797 suppress the CX3CL1/CX3CR1 signaling pathway at P14

(A) Immunofluorescence staining of CX3CL1 in the retinas of the AZD8797 treated mice, as indicated by the red arrow. **(B)** Immunofluorescence staining of CX3CR1 in the retinas after AZD8797 treatment at P14, which indicated by the red arrow. **(C,D and E)** the expression levels of CX3CL, CX3CR1 and NF-κB protein were analyzed by western blot assay. NF-κB and statistical line chart of gray value. (Scale:20μm) (*P < 0.05, **P < 0.01, ****P < 0.0001, for differences compared with the normal control, $^{\#}P$ < 0.05, $^{\#\#}P$ < 0.01, $^{\#\#\#}P$ < 0.001, for differences between animal groups, n = 6.)